Mitochondria as the Primary Target of Resveratrol-Induced Apoptosis in Human Retinoblastoma Cells

Dhruv Sareen,[1,2] *Paul R. van Ginkel,*[2] *Jennifer C. Takach,*[1,2] *Ayesha Mohiuddin,*[2] *Soesiawati R. Darjatmoko,*[2] *Daniel M. Albert,*[2] *and Arthur S. Polans*[1,2]

Purpose. To determine the molecular mechanisms by which resveratrol induces retinoblastoma tumor cell death.

Methods. After resveratrol treatment, Y79 tumor cell viability was measured using a fluorescence-based assay, and proapoptotic and antiproliferative effects were characterized by Hoechst stain and flow cytometry, respectively. Mitochondrial transmembrane potential ($\Delta\Psi_m$) was measured as a function of drug treatment using 5,5′,6,6′-tetrachloro-1,1′,3,3′-tetraethylbenzamidazolocarbocyanin iodide (JC-1), whereas the release of cytochrome *c* from mitochondria was assayed by immunoblotting and caspase activities were determined by monitoring the cleavage of fluorogenic peptide substrates.

Results. Resveratrol induced a dose- and time-dependent decrease in Y79 tumor cell viability and inhibited proliferation by inducing S-phase growth arrest and apoptotic cell death. Preceding cell death, resveratrol evoked a rapid dissipation of $\Delta\Psi_m$. This was followed by the release of cytochrome *c* into the cytoplasm and a substantial increase in the activities of caspase-9 and caspase-3. Additionally, in a cell-free system, resveratrol directly induced the depolarization of isolated mitochondria.

Conclusions. These results demonstrate that resveratrol, a nontoxic natural plant compound, inhibits Y79 cell proliferation and stimulates apoptosis through activation of the mitochondrial (intrinsic) apoptotic pathway and may warrant further exploration as an adjuvant to conventional anticancer therapies for retinoblastoma. (*Invest Ophthalmol Vis Sci.* 2006;47:3708–3716) DOI:10.1167/iovs.06-0119

Retinoblastoma (RB) is the most common intraocular malignancy of infancy and childhood. It represents approximately 4% of all pediatric malignancies in developed countries.[1–3] It is estimated that 250 to 300 new cases of RB are diagnosed in the United States each year and that 5000 cases are diagnosed worldwide.[2,4] These neoplasms arise from loss or mutation of both alleles of the RB tumor-suppressor gene (*RB1*) in the developing retina. In nonheritable RB, both *RB1* alleles are inactivated somatically in a single retinoblast. In heritable RB, one allele is mutated in the germline, and loss or mutation of the second allele occurs in developing retinal cells, typically resulting in multifocal bilateral disease.

With early diagnosis and treatment, the survival rate is greater than 90% in the United States and Western Europe, but vision is often lost in one or both eyes. Patients with a germline RB mutation are at substantial risk for a second high-grade malignancy.[5] The secondary malignancy can lead to metastatic disease after extraocular dissemination to the orbit and death in 50% of affected children worldwide, often as a result of late detection. Traditionally, RB has been treated by enucleation and radiotherapy (external beam and plaque).[4,6] Alternative current treatment modalities include chemotherapy, laser photocoagulation therapy, and cryotherapy.[4,7,8] Although efficacious, these treatment modalities are more effective with smaller tumors. These existing concerns necessitate the development of novel therapeutic modalities.

Recently, a number of strategies have been tested preclinically, including the use of vitamin D analogs,[9,10] viral therapy,[11] and suicide gene therapy.[12] In recent years, resveratrol (RES), a naturally occurring polyphenol highly enriched in grapes, peanuts, red wine, and a wide variety of food sources, has attracted considerable interest because of its cardioprotective, antiaging, and cancer chemopreventive effects.[13,14] RES has been shown to inhibit tumor initiation, promotion, and progression in a variety of cell culture systems[15] and animal models of skin and mammary carcinogenesis.[16,17]

Cell cycle deregulation has been associated with the development of cancer. As a strategic response, anticancer agents have been sought that can modulate cell cycle–associated proteins to arrest tumor proliferation, mostly in an irreversible way, leading to apoptosis.[18,19] The protein product of the *RB1* gene, retinoblastoma tumor-suppressor protein (pRb), and cyclin-dependent kinases (CDKs), their activators (cyclins), and their associated inhibitors form a network of complexes driving cells in and out of the cell cycle phases. Data from various in vitro studies indicate that the antiproliferative effects of RES are mediated through cell-cycle arrest. These effects have been associated with changes in the expression and phosphorylation of pRb,[20–22] and the deregulation of various cyclins, CDKs, and CDK inhibitors.[19,23,24] Although RES-induced alterations in the activities of pRb and cell-cycle regulatory proteins have been documented, there are considerable mechanistic differences in the way the cell cycle is altered between various cell types. No coherent mode of action has yet been determined for RES.

A novel chemotherapeutic approach explored in recent years is based on cytotoxic molecules that perturb mitochondria, thereby circumventing upstream proapoptotic pathways that may be mutated or lacking in cancer cells.[25,26] The mitochondrial-dependent apoptotic pathway is initiated through the disruption of the mitochondrial membrane potential directly or indirectly. This disruption leads to the release of cytochrome *c* and the formation of the apoptosome complex, consisting of cytochrome *c*/caspase-9/Apaf-1 and activation of

From the Departments of [1]Biomolecular Chemistry and [2]Ophthalmology and Visual Sciences, University of Wisconsin School of Medicine and Public Health, Madison, Wisconsin.

Supported by National Institutes of Health Grant RO1 CA103653 (ASP); the Retina Research Foundation (ASP); and the National Research Service Award T32 GM07215–30 (JCT).

Submitted for publication February 3, 2006; revised March 31, 2006; accepted June 23, 2006.

Disclosure: **D. Sareen**, None; **P.R. van Ginkel**, None; **J.C. Takach**, None; **A. Mohiuddin**, None; **S.R. Darjatmoko**, None; **D.M. Albert**, None; **A.S. Polans**, None

The publication costs of this article were defrayed in part by page charge payment. This article must therefore be marked "*advertisement*" in accordance with 18 U.S.C. §1734 solely to indicate this fact.

Corresponding author: Arthur S. Polans, Department of Ophthalmology and Visual Sciences, University of Wisconsin School of Medicine and Public Health, Room K6/466 Clinical Sciences Center, 600 Highland Avenue, Madison, WI 53792; aspolans@facstaff.wisc.edu.

the caspase cascade and resulting in the morphologic and biochemical changes in the cell that lead to apoptosis.

Recently, RES has been to shown to inhibit several important enzymes involved in carcinogenesis: the mitochondrial electron transport chain proteins, NADH/ubiquinone oxidoreductase (complex-1),[27] F0-F1 ATPase,[28–30] and other cellular enzymes such as DNA polymerases α and β,[31,32] cyclooxygenases (COX-1 and COX-2),[15,33,34] human cytochrome P450 isoenzymes such as CYP 1A1,[35] and NRH/quinone oxidoreductase 2 (NQO2), also known as quinone reductase-2 (QR-2).[36] NQO2 has been identified as a resveratrol-targeting protein using a resveratrol affinity column and co-crystallized in complex with resveratrol.[36,37] It is a cytosolic flavoprotein that catalyzes the reductive metabolism of quinones and their derivatives to protect cells against redox cycling and oxidative stress.[38]

Although we have seen that RES is a relatively nontoxic anticancer agent in vivo and that it inhibits different stages of tumor growth, the molecular mechanism of its anticancer activity is still not well defined. Our data demonstrate that RES can induce apoptotic death in human retinoblastoma Y79 cells. This occurs through a mechanism that involves the deregulation of the cell cycle machinery, direct depolarization of mitochondria, and activation of mitochondria-mediated, caspase-dependent apoptotic signaling cascades. Understanding the molecular signaling mechanisms of RES may facilitate the development of therapeutic interventions for the treatment of RB.

Materials and Methods

Reagents

The human Y79 retinoblastoma and SK-N-AS neuroblastoma cell lines were obtained from Daniel M. Albert (Madison, WI). RES (Cayman Chemicals, Ann Arbor, MI) was dissolved in sterile dimethylsulfoxide (DMSO) as a stock solution of 200 mM and further diluted in cell culture media. Complete protease inhibitor cocktail, 0.25% trypsin-EDTA solution, and all other chemicals were purchased for use as reagents (Sigma-Aldrich Chemical Co., St. Louis, MO).

Cell Culture

Y79 cells were grown in Iscove modified Dulbecco medium (IMDM; Cambrex Biosciences, Walkersville, MD) supplemented with 25% vol/vol fetal bovine serum (FBS; Atlanta Biologicals, Norcross, GA), 2 mM L-glutamine, 100 U/mL penicillin G, 100 mg/mL streptomycin sulfate, and 0.25 mg/mL amphotericin B.

SK-N-AS cells were cultured in RPMI medium supplemented with 10% vol/vol FBS, 100 U/mL penicillin G, 100 mg/mL streptomycin sulfate, and 0.25 mg/mL amphotericin B. Cultures were maintained at 37°C in a 95% O_2/5% CO_2 atmosphere. Cells were treated with RES in DMSO or 0.1% DMSO alone for various times, as indicated in the figure legends, and fresh RES and culture medium were changed every 48 hours.

Tumor Cell Viability

For cell viability analysis, Y79 cells were seeded in 6-well plates (2×10^5 cells/well in 2 mL medium), and SK-N-AS cells were seeded in 96-well plates (2×10^4 cells/well in 0.2 mL medium) and subsequently were incubated for different times in the presence of RES or vehicle alone. RES was added at appropriate concentrations to the culture medium 1 day after plating, and samples were analyzed at particular time points each day. At the end of the treatment, dye (CellTiter-Blue; Promega, Madison, WI) was added according to the manufacturer's instructions. The assay used (CellTiter-Blue Cell Viability Assay; Promega) is a fluorometric assay based on the metabolic capacity of live cells to reduce the indicator dye resazurin to a highly fluorescent resorufin. Fluorescence was measured at excitation/emission wavelengths of 560/590 nm with the use of a fluorescence plate reader (Molecular Dynamics, Sunnyvale, CA). The experiment was performed with triplicate wells seeded for each condition. For cell regression analysis, cell viability was determined by the trypan blue exclusion test. Viable cells excluded the dye, whereas dead cells absorbed the dye. A 50% cell suspension was mixed with 50% trypan blue isotonic solution, and the viable cells were counted with a hemocytometer under a light microscope.

Determination of Apoptotic Cell Morphology

Y79 cells were treated at a density of 2×10^5 cells/mL with 100 μM RES. At 24, 48, 72, and 96 hours after treatment, cells were seeded into 8-well poly-L-lysine–coated chamber slides (LabTek II; Nalge Nunc International, Naperville, IL), fixed with 4% paraformaldehyde/5% sucrose in 0.1 M Na-phosphate buffer for 45 minutes, washed with PBS, stained with 1 μg/mL cell permeable, minor groove-binding dye that fluoresces bright blue on binding to DNA (Hoechst 33528; Molecular Probes, Eugene, OR) in PBS for 60 minutes at 37°C, and viewed under a fluorescence microscope (Carl Zeiss, Oberkochen, Germany). A nucleus with condensed chromatin and a discontinuous nuclear envelope observed with the dye used (Hoechst 33528; Molecular Probes) is a hallmark of an apoptotic cell. The percentage of apoptotic cells was calculated by counting the number of apoptotic cells in a viewing field relative to the total number of cells. Cell counts were determined over five viewing fields and averaged.

Cell Cycle Distribution Analysis

Cells were plated in 10-cm culture dishes at concentrations determined to yield 60% to 70% confluence within 24 hours. Cells were then treated with either DMSO (0.1%) or RES (50 and 100 μM). After 48 hours of treatment, cells were harvested, washed with PBS, and fixed in 70% ethanol for 45 minutes at room temperature (RT). Fixed cells were washed again with PBS and incubated in 0.04% pepsin (Sigma) in 0.1 N HCl for 20 minutes at RT. After the addition of PBS containing 0.5% Tween-20 and 0.1% BSA (PBS-TB), nuclei were pelleted and resuspended in 2 N HCl for 30 minutes at 37°C. The suspension was neutralized by the addition of 2 vol 0.1 M sodium borate. Nuclei were washed with PBS-TB and then incubated with 75 μM propidium iodide (PI) in PBS-TB overnight at 4°C. PI is a fluorescent dye that intercalates in the DNA helix with a resultant increase in fluorescence, and it is used to quantitatively assess DNA content. After incubation with 20 μg/mL RNase A for 20 minutes at 37°C, DNA content was then analyzed using a flow cytometer (FACStation; Becton Dickinson, San Jose, CA) equipped with computer software (ModFit [Verity Software House, Topsham, ME] and CellQuestPro [Becton Dickinson]).

Immunoblotting

Cell cultures were washed twice with PBS and lysed in ice-cold lysis buffer (50 mM Tris-HCl [pH 7.5], 150 mM NaCl, 0.5% Nonidet P-40, 1 mM PMSF, 1 mM NaF, 1 mM DTT, and 4 mg/mL complete protease inhibitor cocktail). Protein concentration was determined in cell lysates using the Bradford assay (Bio-Rad protein assay kit; Bio-Rad, Hercules, CA). Aliquots of 15 μg protein were mixed with sodium dodecyl sulfate (SDS) sample buffer, denatured, and separated by SDS-PAGE using 15% polyacrylamide gels. Proteins were transferred to PVDF membranes by electroblotting. Membranes were blocked for 1 hour at room temperature with 5% (wt/vol) nonfat milk and 5% BSA in TBS-T [50 mM Tris-HCl (pH 7.5), 150 mM NaCl, and 0.2% Tween-20]. Blots were incubated with primary antibodies; GAPDH (1:100,000; Biogenesis Inc., Poole, UK), cytochrome *c* (1:1000; clone 7H8.2C12, BD PharMingen, San Diego, CA), or NQO2 (1:1000; N-15, Santa Cruz Biotechnology, Santa Cruz, CA). Incubations were followed by TBS-T washes, incubation with secondary antibodies, horseradish peroxidase–conjugated goat anti–mouse IgG and rabbit anti–goat IgG (1:10,000; Upstate Cell Signaling, Charlottesville, VA), and further TBS-T washes. Immunoreactive proteins were visualized by the enhanced chemiluminescence (ECL) procedure according to the manufacturer's protocol (Amersham Pharmacia, Piscataway, NJ).

NQO2 mRNA analysis

Total RNA was isolated from cells with an isolation kit (RNeasy mini RNA; Qiagen, Chatsworth, CA) according to the manufacturer's instructions. Samples were DNAse I treated and reverse transcribed using Moloney murine leukemia virus (MMLV) and a mixture of oligo-dT and random primers (Promega), followed by RNase H treatment. Quantitative real-time PCR was performed with SYBR mix (Bio-Rad) using NQO2-specific primers (sense, 5′-TGAAGGGCTGGATGGATAGG-3′; antisense, 5′-CCTGGAGCAAACCGGAATC-3′) and β-glucuronidase (GUS)–specific primers (sense, 5′-GGAATTTTGCCGATTTCATGA-3′; antisense, 5′-AGGAACGCTGCACTTTTTGG-3′) as an internal standard (iCycler; Bio-Rad). Relative expression levels and ranges were calculated according to the comparative method, as described previously.[39]

Isolation of Mitochondria

Y79 cells were washed twice in mitochondrial extraction buffer (10 mM HEPES, pH 7.5, containing 200 mM mannitol, 70 mM sucrose, and 1 mM EGTA) and were resuspended in 10 vol extraction buffer (Mitochondrial Isolation Kit; Sigma). Cells were homogenized with 50 to 60 passes of a PTFE pestle in a 15-mL volume homogenizer (Potter-Elvehjem, Dusseldorf, Germany). Nuclei and intact cells were removed by centrifugation using a table top centrifuge at 600*g* for 5 minutes. The supernatant was centrifuged again at 11,000*g* for 10 minutes, and this supernatant was stored as the cytosolic fraction. The pellet was resuspended in 10 vol extraction buffer, and the centrifugation steps of 600*g* and 11,000*g* were repeated. The final pellet (mitochondrial fraction) was resuspended in assay buffer containing 20 mM MOPS, pH 7.5, 110 mM KCl, 10 mM ATP, 10 mM $MgCl_2$, 10 mM sodium succinate, and 1 mM EGTA and was stored for short periods on ice until further analysis.

Mitochondrial Transmembrane Potential ($\Delta\Psi_m$)

Changes in mitochondrial membrane potential were analyzed using a spectrofluorometer (RP 5301-PC; Shimadzu Scientific, Columbia, MD) and a mitochondria-selective dye (JC-1; Cell Technology, Mountain View, CA).[40,41] JC-1 is a lipophilic cation, which in a reaction driven by $\Delta\Psi_m$ in normal polarized mitochondria assembles into a red fluorescence-emitting dimer forming J-aggregates. However, the monomeric form present in cells with depolarized mitochondrial membranes emits only green fluorescence.

Cells. Cells (2×10^5) were treated with 0.1% DMSO (vehicle) or RES for 15 minutes at 37°C. After removing the drugs, the cells were stained with JC-1 for 15 minutes at 37°C, washed once with assay buffer, and analyzed in assay buffer using a spectrofluorometer to detect green fluorescence at excitation/emission wavelengths of 485/530 nm and red fluorescence at excitation/emission wavelengths of 550/595 nm. The ratio of red to green fluorescence intensity was determined for each sample as a measure of $\Delta\Psi_m$. As a control to verify that RES does not interfere with the uptake of JC-1, cells were preloaded with JC-1 for 15 minutes at 37°C, washed twice with assay buffer, treated with drugs, washed with assay buffer, and analyzed as described above.

Isolated Mitochondria. Twenty micrograms of protein from isolated mitochondria were treated with 0.1% DMSO or RES for 15 minutes at 37°C. Mitochondria were pelleted by centrifugation at 11,000*g* for 10 minutes, and the drugs were removed. The mitochondria were then stained with JC-1 for 15 minutes at 37°C and were washed with assay buffer, and JC-1 red fluorescence intensity was analyzed on a spectrofluorometer, as described. Valinomycin, a potassium ionophore, carbonyl cyanide-*p*-(trifluoromethoxy)phenylhydrazone (FCCP), a protonophore, and sodium azide (Sigma), a mitochondrial complex IV inhibitor, were uncouplers of mitochondrial oxidative phosphorylation, significantly dissipated $\Delta\Psi_m$, and served as controls.

Determination of Caspase Activation

Y79 cells (1×10^6) were seeded on 10-cm culture dishes and treated with 0.1% DMSO or RES for 24, 48, and 72 hours. The activities of caspase-9 and caspase-3 were determined as previously described.[42] Briefly, after the induction of apoptosis, Y79 cells were pelleted and resuspended in lysis buffer (10 mM Tris-HCl, 10 mM NaH_2PO_4, pH 7.5, 130 mM NaCl, 1% [vol/vol] Triton X-100). Protein concentration was measured according to the manufacturer's instructions (Bio-Rad). Protein (40 μg and 100 μg) was incubated with fluorogenic peptide substrates, *Ac*-Asp-Glu-Val-Asp-amido-4-methyl-coumarin (*Ac*-DEVD-AMC; BD PharMingen, San Diego, CA) for caspase-3 and *Ac*-Leu-Glu-His-Asp-amido-4-trifluoromethyl-coumarin (*Ac*-LEHD-AFC; MP Biomedicals, Irvine, CA) for caspase-9, respectively, in reaction buffer (20 mM HEPES-KOH, 10% glycerol, 2 mM DTT) for 30 to 60 minutes at 37°C. The uncleaved peptide substrates produced a blue fluorescence. Cleavage by active caspases resulted in the release of free fluorochrome (AFC or AMC), producing a yellow-green fluorescence that was monitored on a spectrofluorometer by setting the wavelengths to $\lambda_{ex} = 400$ nm, $\lambda_{cm} = 505$ nm (*Ac*-LEHD-AFC), and $\lambda_{ex} = 380$ nm, $\lambda_{em} = 440$ nm (*Ac*-DEVD-AMC). The amount of yellow-green fluorescence produced on cleavage is proportional to the amount of active caspase-9 or caspase-3 present in the samples. The increase in caspase activities was determined by comparing the levels of the RES-treated cells with untreated controls.

Cytochrome *c* Release

Cytosolic and mitochondrial fractions were analyzed for cytochrome *c* content by immunoblotting.

Cells. Briefly, Y79 cells (~5×10^6) were treated with vehicle or RES. Cells were harvested and washed twice with cold PBS and sedimented by centrifugation. Cell pellets were resuspended in permeabilization buffer (0.25 M sucrose, 20 mM HEPES, pH 7.4, 10 mM KCl, 1 mM $MgCl_2$, 1.5 mM Na-EGTA, 1.5 mM Na-EDTA, 1 mM $MgCl_2$, 1 mM DTT, 0.1 mM PMSF, and 25 μg/mL digitonin containing protease inhibitors) for 8 minutes at 4°C. Permeabilized cells were centrifuged (600*g*, 10 minutes) at 4°C. Supernatants were centrifuged again (11,000*g*, 10 minutes). The supernatant of this centrifugation was saved as the cytosolic fraction. The pellet, which contained membranes and subcellular organelles, was washed with PBS, resuspended in permeabilization buffer, and sonicated in a water bath for 2 minutes This final protein extract constituted the mitochondrial fraction.

Isolated Mitochondria. Isolated mitochondria (20 μg protein) were treated with 0.1% DMSO or RES at 37°C in assay buffer. Mitochondria were pelleted by centrifugation at 11,000*g* for 10 minutes, and the supernatant fraction was saved for cytochrome *c* detection. The pellet was washed with assay buffer and saved as the mitochondrial fraction.

Protein concentrations were measured with the use of a protein assay kit (Bio-Rad). Proteins were separated on a 15% SDS–polyacrylamide gel, transferred to PVDF membranes, probed with anti–cytochrome *c* antibody (7H8.2C12), and visualized with an ECL detection system (Amersham Pharmacia), as described.

Results

Dose- and Time-Dependent Effects of Resveratrol on the Growth and Cytotoxicity of Human Retinoblastoma Y79 Cells In Vitro

To examine the antitumor activity of RES in human retinoblastoma Y79 cells, exponentially dividing cells were treated with increasing concentrations of RES, and cell viability was measured. RES caused marked growth inhibition and significantly decreased cell viability in a time- and concentration-dependent manner (Fig. 1A). After 48 hours of treatment, RES had an IC_{50} of 170 μM. Treatment of dense Y79 cultures with RES resulted in a time-dependent decrease in the number of viable cells analyzed by the trypan blue exclusion assay (Fig. 1B). No viable cells were detectable after 6 days of exposure to RES.

We were interested in determining whether RES induces apoptosis, contributing in part to its growth-inhibitory effects.

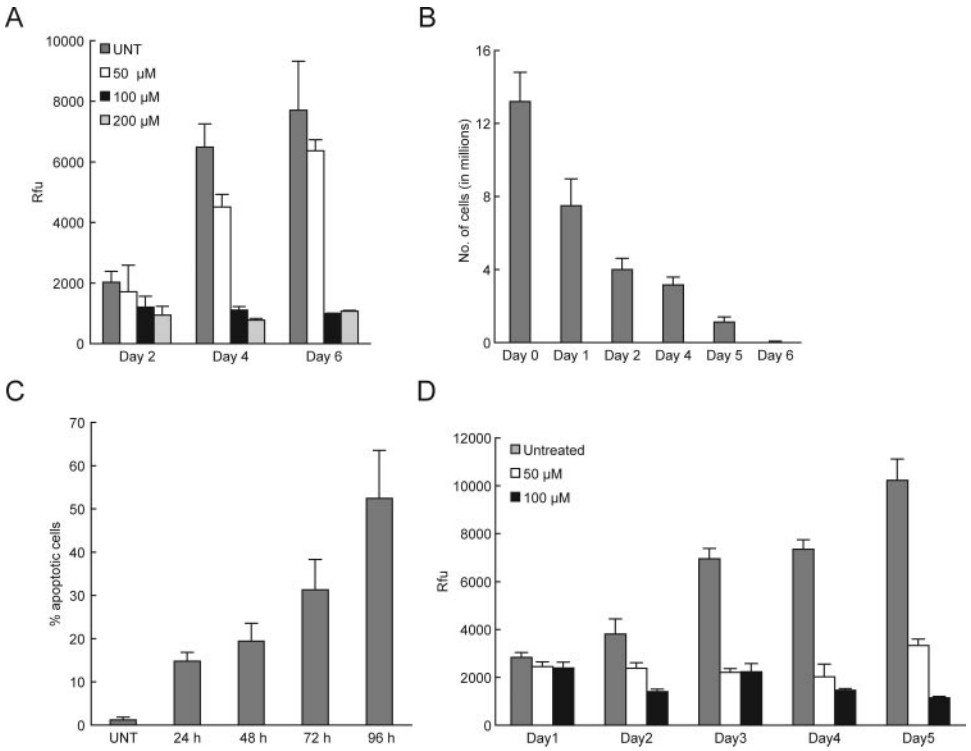

FIGURE 1. RES causes dose- and time-dependent growth inhibition and induces apoptosis of Y79 cells in vitro. (**A**) Growth suppression effects of RES on Y79 cells treated with 0.1% DMSO vehicle control (UNT) or 50, 100, and 200 μM RES. Cell viability was measured at the end of 2, 4, and 6 days of treatment. IC_{50} = 170 μM was the concentration of agent at 48 hours that reduced cell numbers by 50% under the experimental conditions. (**B**) Regression of exponentially dividing dense Y79 cell cultures treated with 200 μM RES for 6 days. The number of viable cells was determined daily in triplicate using the trypan blue dye exclusion assay. (**C**) Y79 cells were treated with 0.1% DMSO vehicle (UNT) or 100 μM RES for 24, 48, 72, or 96 hours and were stained with Hoechst 33528. Nuclear morphology was examined by fluorescence microscopy. Cells exhibiting hallmark characteristics of apoptotic nuclei were counted, and the number of apoptotic cells was determined as a percentage of the total number of cells in a viewing field. Value at each time point was averaged over five different viewing fields. (**D**) Cell viability of SK-N-AS cells was measured as a function of RES treatment (IC_{50} = 100 μM). (**A–D**) Mean ± SD of triplicate samples. Results are representative of one of three independent experiments.

Y79 cells were treated with DMSO alone or with 100 μM RES and stained with Hoechst 33528, and morphologic changes were examined under a fluorescence microscope. Y79 cells exhibiting typical morphologic features of apoptosis, such as chromatin condensation and nuclear disintegration, increased in a time-dependent manner when treated with RES. Results are represented as percentage of apoptotic cells, which increased from 2% in control cells to 52% after treatment with RES for 96 hours (Fig. 1C), suggesting that RES has a proapoptotic effect in Y79 cells.

RB is a member of the small cell tumors of childhood that include neuroblastoma. Neuroblastoma and RB metastases are almost indistinguishable, often requiring immunohistochemical stains for definitive identification, and treatment of RB is based on protocols for neuroblastoma. Figure 1D demonstrates that RES has the same effect on the viability of human SK-N-AS neuroblastoma cells as observed for Y79.

Effects of RES on Y79 Cell Cycle Progression and Proliferation

Although it was apparent that RES was cytotoxic to Y79 cells, the sustained growth-inhibitory effects observed by the cell viability assay indicate that RES might also affect cell proliferation. To assess whether RES induced growth inhibition, we evaluated the effect of RES on cell cycle progression in exponentially dividing cultures of Y79 cells. Subconfluent cultures were treated with DMSO alone or with RES and were analyzed by flow cytometry. RES significantly increased the appearance of the sub-G_1 fraction, from 1.5% in control conditions to 4.7% and 13.1% after 50 μM and 100 μM RES treatment, respectively (Fig. 2A). The increase in the sub-G_1 fraction represents an increase in hypodiploid DNA content from apoptotic DNA fragmentation, indicating an increase of RES-induced apoptotic cell death and corroborating results obtained by Hoechst stain. The percentage of cells in G_0/G_1, S, and G_2-M phases were calculated and are represented as histograms (Fig. 2B). RES caused an increased cell population in the S-phase of the cell cycle (43% in control vs. 82% and 70% with 50 and 100 μM RES, respectively) and a concomitant decreased cell population in the G_1 phase (47% in control vs. 9% and 20% with 50 and 100 μM RES, respectively). The results given in Figures 1 and 2 demonstrate that RES inhibits tumor cell growth by exerting both antiproliferative and proapoptotic effects on Y79 cells.

Relationship between Effects of Resveratrol and NQO2 Levels in Y79 Cells

Recently, NQO2 (QR2) has been identified as a resveratrol-targeting protein, and RES has been shown to be a potent inhibitor of NQO2/QR2 activity in vitro with a dissociation constant of 35 nM.[36,37] To examine a putative NQO2-dependent mechanism through which RES could impart its effects contributing to apoptotic death in Y79 cells, we analyzed NQO2 protein expression levels in Y79 cells by Western blot analysis and mRNA levels by quantitative real time-PCR (qRT-PCR). Immunoblot analysis showed that Y79 cells had undetectable levels of NQO2 protein (Fig. 3A) compared with SK-N-AS neuroblastoma cells. Even though Y79 cells lacked detectable NQO2, both Y79 and SK-N-AS cells were equally sensitive to RES-induced cell death in vitro (Figs. 1A, 1D), indicating that NQO2 is not likely the primary target of RES. A mouse liver extract was used as a positive control for NQO2 protein expression. These findings were confirmed by qRT-PCR, which showed low levels of NQO2 transcript in Y79 cells. Levels of NQO2 mRNA were approximately 26-fold higher in SK-N-AS cells than in Y79 cells (Fig. 3B).

Resveratrol-Induced Alterations in $\Delta\Psi_m$

As an alternative to the NQO2-mediated mechanism of RES-induced cytotoxicity and apoptosis, its effects on the intrinsic mitochondrial apoptotic pathway were explored in Y79 cells.

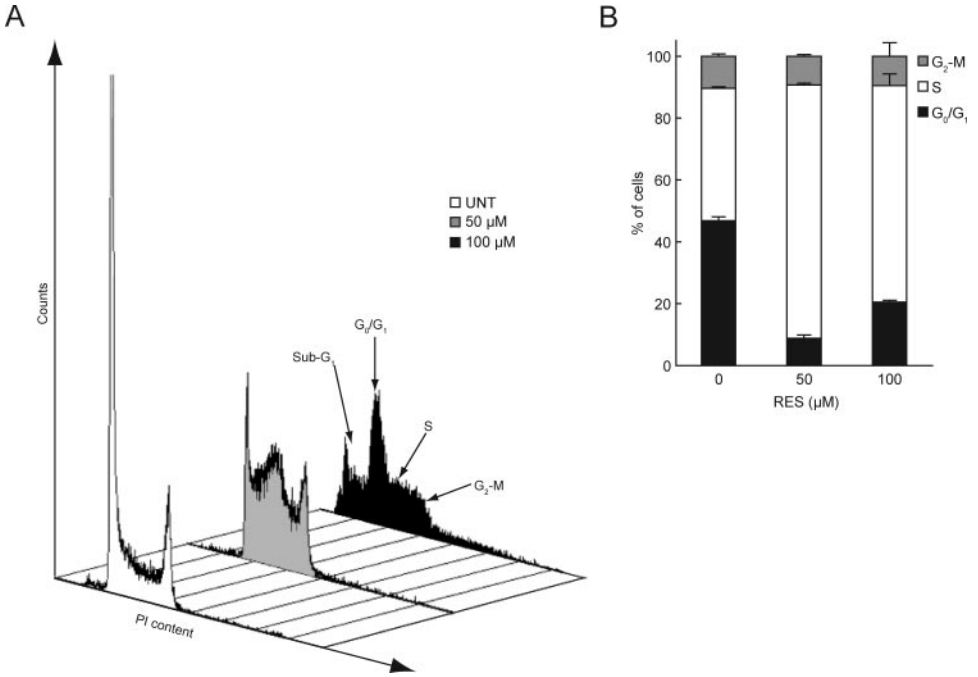

FIGURE 2. RES affects Y79 cell cycle progression and blocks proliferation. (**A**) Y79 cells were treated with 0.1% DMSO (UNT) or 50 and 100 μM RES for 48 hours. Harvested cells were fixed and stained with PI, followed by flow cytometric analysis. Cells with hypodiploid DNA content (sub-G_1) represent fractions undergoing apoptotic DNA fragmentation. An increasing fraction of cells in the S-phase could be observed with RES treatment. (**B**) The percentage of cells in the G_0/G_1, S, and G_2-M phases were analyzed and are represented within the histograms. (**A**, **B**) Mean ± SD of duplicate samples. Results are representative of one of two independent experiments.

Chemically induced apoptosis mediated by the mitochondria/caspase-9 activation pathway is often, though not always, associated with the collapse of $\Delta\Psi_m$ as a result of leakiness of the inner mitochondrial membrane.[43] To delineate this mechanism, the lipophilic cation JC-1 was used to determine whether RES induces alterations in $\Delta\Psi_m$.

Fifteen minutes after RES exposure, a dramatic dose-dependent decrease in the ratio of red-green fluorescence intensity could be observed, indicating rapid depolarization of mitochondrial membranes. Significant depolarization with greater than a fourfold decrease in $\Delta\Psi_m$ could be observed after treatment with 50 μM RES (Fig. 4A). FCCP and valinomycin, known agents that depolarize mitochondrial membranes, were used as positive controls. To assess whether the loss in membrane potential was sustained, the RES-induced disruption of $\Delta\Psi_m$ was determined after a time-course treatment. Y79 cells displayed a sustained loss of $\Delta\Psi_m$ for 24 hours after the addition of 100 μM RES (Fig. 4B). These results were confirmed with the use of a second mitochondrial membrane potential selective dye, tetramethylrhodamine methyl ester perchlorate (TMRM) (data not shown). To demonstrate that RES did not alter JC-1 staining by interfering with its uptake mechanism, JC-1 was preloaded in Y79 cells before drug treatment. As described earlier, RES induced a rapid, dose-dependent loss of $\Delta\Psi_m$ (Fig. 4C). Therefore, in accordance with the sensitivity of Y79 cells to RES-induced apoptosis, these results suggest that a collapse of $\Delta\Psi_m$ is an early event in RES-induced apoptosis.

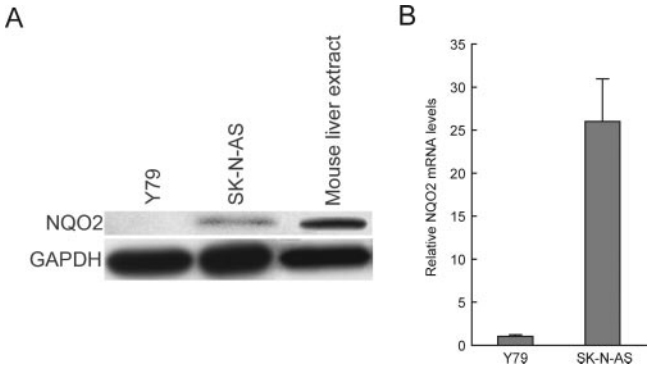

FIGURE 3. RES-induced cell death is not dependent on NQO2 protein and mRNA levels in Y79 cells. (**A**) The protein levels of NQO2 were determined in Y79 and SK-N-AS cell lysates and were compared with a positive control from mouse liver extract. Equal loading was determined by staining for GAPDH. (**B**) Real-time PCR confirmed the low levels of NQO2 mRNA in Y79 cells (normalized to 1) when compared with SK-N-AS cells. (**B**) Mean ± SD of triplicate samples. (**A**, **B**) Results are representative of one of two independent experiments.

Effects of Resveratrol on Membrane Potential in Isolated Mitochondria

Because RES can cause the loss of $\Delta\Psi_m$ in cells, JC-1 stain was used to determine whether RES might directly target mitochondria in a cell-free system. Freshly isolated mitochondria were incubated with JC-1 dye after treatment with various doses of RES. The intensity of red fluorescence was monitored, with a decrease signifying the inability of the dye to form J-aggregates (red) in the mitochondria attributed to a decrease in $\Delta\Psi_m$. RES was found to directly cause a concentration-dependent loss in $\Delta\Psi_m$ in isolated mitochondria that was rapid (within 10 minutes) (Fig. 5). A difference could be seen in $\Delta\Psi_m$ between whole cells and isolated mitochondria as a function of RES concentration. The changes in mitochondrial potential after RES treatment in isolated mitochondria could be observed starting at 1 μM, compared with 50 μM in whole cells (compare Figs. 4A and 5). At 5 μM RES, the J-aggregates were almost undetectable in the isolated mitochondria, indicating complete loss of $\Delta\Psi_m$.

Resveratrol-Induced Mitochondrial Translocation of Cytochrome *c*

Mitochondria play an essential role in apoptosis triggered by chemical agents. The mitochondrial response includes the release of cytochrome *c* into the cytosol. In the cytosol, cytochrome *c* binds to Apaf-1, allowing the recruitment of caspase-9 and the formation of an apoptosome complex, resulting in caspase-3 activation and execution of cell death.[44] To determine whether RES initiates this cell death mechanism, we tested whether it triggers the release of cytochrome *c* from the mitochondria. After treatment with 0.1% DMSO or 100 μM RES, Y79 cells were fractionated into separate cytosolic and mitochondrial fractions. The

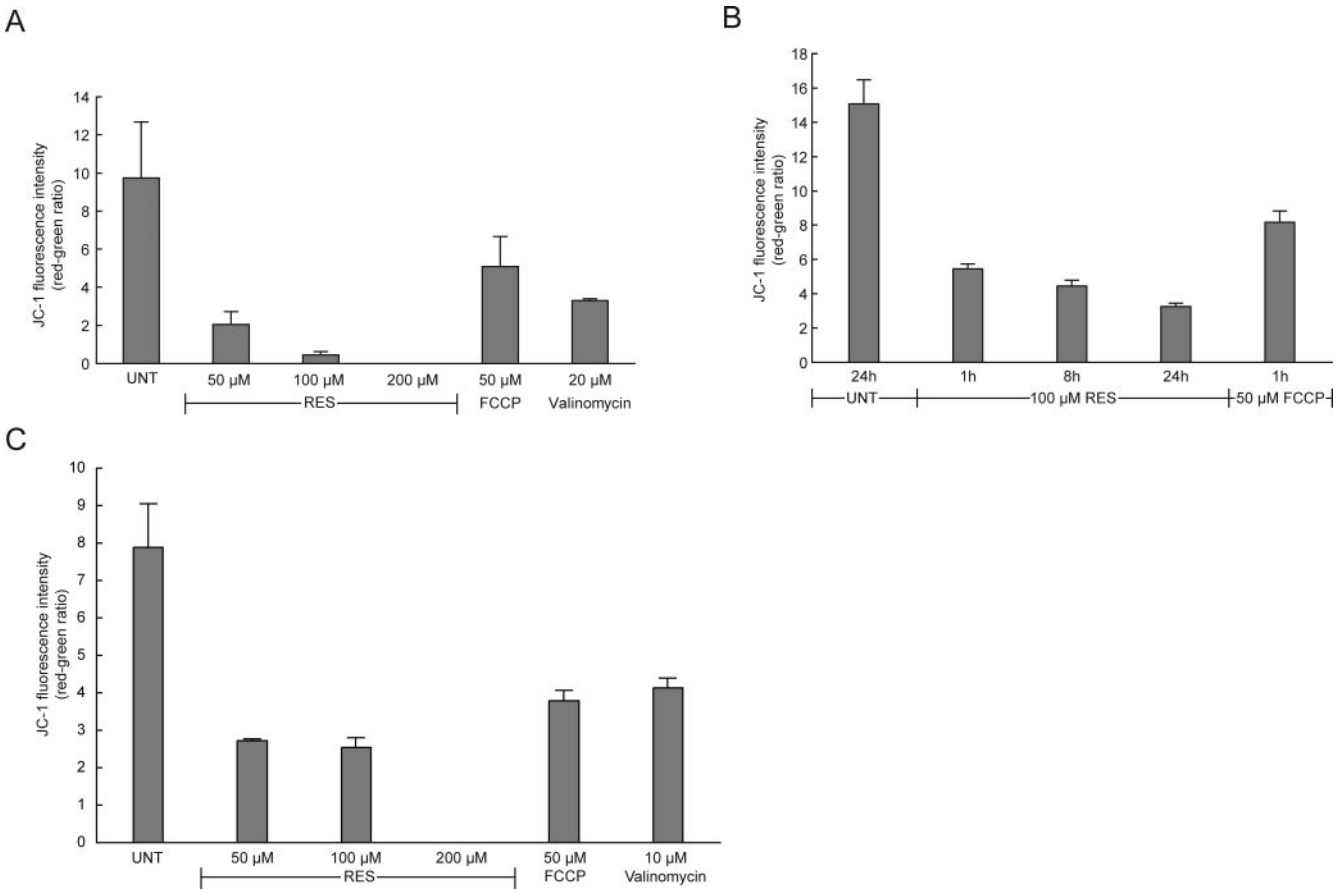

FIGURE 4. RES disrupts normal mitochondrial transmembrane potential. (**A**) Y79 cells were treated with 0.1% DMSO (UNT) or 50, 100, and 200 μM RES for 15 minutes and were stained with JC-1. (**B**) Cells were treated with 0.1% DMSO (UNT) or 100 μM RES for various periods and stained with JC-1. (**C**) As a control to verify JC-1 uptake, cells were prestained with JC-1 and subsequently treated with 0.1% DMSO (UNT) or 50, 100, and 200 μM RES for 15 minutes. Changes in $\Delta\Psi_m$ were measured spectrofluorometrically. As positive controls, cells were treated with FCCP and valinomycin. (**A–C**) Mean ± SD of duplicate samples. Results are representative of one of three independent experiments.

amount of cytochrome *c* release was examined in the cytosolic and mitochondrial fractions by Western blot analysis (Fig. 6A). RES induces a slight increase of cytochrome *c* to the cytosolic compartment as early as 2 hours after treatment. Cytochrome *c* release increased at 24 hours, but after 48 hours RES provoked a large accumulation of this protein in the cytosolic fraction. The

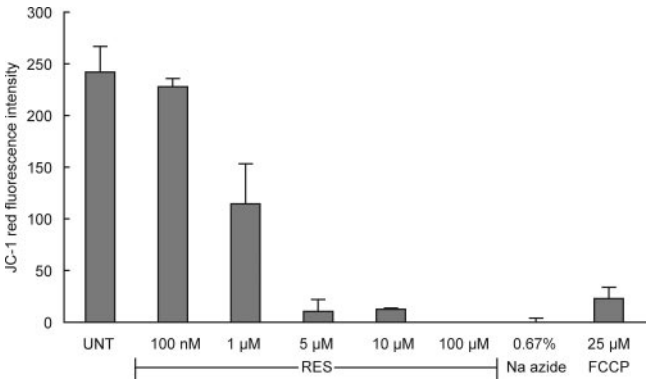

FIGURE 5. RES directly induces depolarization in isolated mitochondria. Mitochondrial fractions were isolated from Y79 cells, incubated with 0.1% DMSO (UNT) or various concentrations of RES for 15 minutes, and stained with JC-1, and changes in $\Delta\Psi_m$ were measured spectrofluorometrically. As positive controls, isolated mitochondrial fractions were treated with 0.67% Na-azide and 50 μM FCCP. Results are representative of one of three independent experiments.

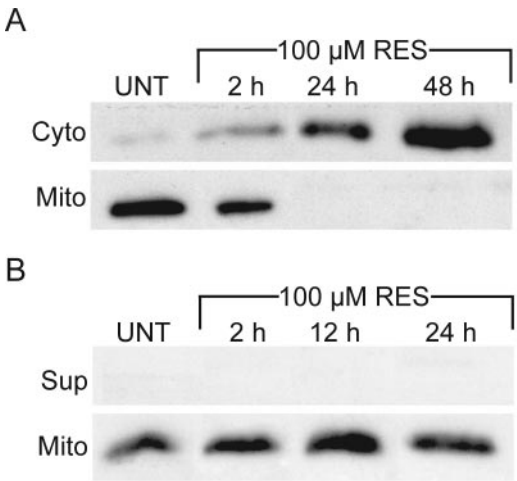

FIGURE 6. RES causes cytochrome *c* release from mitochondria. Intact Y79 cells (**A**) were treated with 0.1% DMSO (UNT) or 100 μM RES for 2, 24, and 48 hours. Isolated mitochondria (**B**) were treated with 0.1% DMSO (UNT) or 100 μM RES for 2, 12, and 24 hours. Cytosolic (Cyto) and mitochondrial (Mito) fractions from intact cells, and supernatant (Sup) and mitochondrial (Mito) fractions from isolated mitochondria were prepared and analyzed for cytochrome *c* levels by immunoblotting using an anti-cytochrome *c* antibody. Samples obtained from the time-course of different fractions (Cyto, Sup, or Mito) were adjusted for equal protein loading by determination of concentrations with the Bradford assay. Results are representative of one of two independent experiments.

temporal profile of cytosolic accumulation of cytochrome *c* parallels its release from the mitochondria (shown in the bottom panel of Figure 6A). These results suggest that RES-induced apoptotic death is mediated by mitochondria-dependent signaling pathways. However, RES could not provoke cytochrome *c* release from isolated mitochondria into the supernatant fraction in a cell-free system (Fig. 6B), indicating that other cytosolic factors are involved in cytochrome *c* release after mitochondrial depolarization.

Participation of Caspases-9 and -3 in Resveratrol-Induced Apoptosis

Loss of $\Delta\Psi_m$ and cytochrome *c* release commonly contribute to apoptosis, occurring either as early initiating events before caspase activation or as late downstream consequences of caspase activation.[44,45] Apoptosis is known to be executed by the linked activation of caspases, such as initiators (caspase-8 and caspase-9) and executioners (caspase-3 and caspase-7). To further determine the involvement of caspase-9 and caspase-3 in RES-induced mitochondria-mediated apoptotic cell death, we examined the cleavage of fluorogenic peptide substrates that mimic the target cleavage sites of caspase-9 and caspase-3 in cell lysates. Y79 cells were left untreated or were treated with 50 μM RES, and caspase activities were determined. The fluorometric protease assays show a time-dependent increase in the activities of caspase-9 and caspase-3 in RES-treated cell lysates (Fig. 7), paralleling the time-course profile of cytochrome *c* release. Slight increases in caspase-9 and caspase-3 activities were observed 24 hours after the addition of RES. However, maximum caspase-9 activation was observed well after the beginning of RES-induced changes in $\Delta\Psi_m$ and cytochrome *c* release. Caspase-9 activation increased ~1.8-fold after 48 hours and ~2.4-fold after 72 hours (Fig. 7A). Caspase-3 activity increased ~twofold after 48-hour and more than fivefold after 72-hour treatment (Fig. 7B). Treatment with 100 μM RES resulted in faster responses in caspase-3 and caspase-9 activation, as early as 3 hours after treatment, but the activities peaked at 36 hours and decreased thereafter (data not shown). These results support the hypothesis that RES can provoke an intrinsic mitochondrial-dependent form of apoptosis in Y79 cells by decreasing $\Delta\Psi_m$, increasing cytochrome *c* release, and activating caspase-9 and caspase-3.

Discussion

This is the first study to assess the chemotherapeutic effects of RES and to describe the signaling mechanisms of RES-induced apoptosis in an RB cell line. RB continues to be a challenge, both diagnostically and therapeutically, in medically underdeveloped nations. Methods of chemotherapy have changed the approach to RB in recent years improving the outcome and providing an alternative to external beam radiotherapy. Therapeutic intervention using natural or synthetic agents may be of further help in the management of RB.

Many compounds used in cancer chemotherapy are derived from plant sources, such as paclitaxel, camptothecin, and etoposide.[46] In the search for novel strategies for the treatment of RB, we have attempted to identify the molecular mechanisms involved in RES-induced apoptosis of human retinoblastoma Y79 cells. In the present study, we have shown that RES exerts antiproliferative and proapoptotic effects on Y79 cells, thus decreasing cell viability. Our results show that RES can induce dose- and time-dependent apoptosis in Y79 cells as judged by cell morphology, chromatin condensation, and appearance of a sub-G_1 cell population.

The antiproliferative activity of RES against tumor cell lines of different origins has been extensively characterized.[14,16,47] Previously, in vitro assays demonstrated that RES can inhibit the catalytic activity of tumor-promoting cycloxygenase-1 and -2 (COX-1 and COX-2)[15,33,34] and can prevent DNA synthesis by direct interaction with DNA polymerases α and δ,[31] thus providing possible mechanisms by which RES blocks cell cycle progression. Despite in vitro data on enzyme inhibition, the most relevant mechanism occurring in vivo may involve the deregulation of multiple targets and pathways. RES downregulates COX-2 transcription in breast cancer cells and is thought to act by inhibiting the activation of the transcriptional factor NF-κB, upstream of COX-2 expression.[48] NF-κB regulates the expression of target genes involved in titration of the balance between proliferation and apoptotic stress response. RES was shown to inhibit NF-κB and its target genes, regulating the activity of the upstream mitogen-activated protein kinases (MAPKs), associated with an antiproliferative action and with the induction of cell death.[21,49,50] Our results indicate that RES inhibits Y79 cell proliferation by inducing S-phase growth arrest, which is confirmed by previous observations from other investigators in various tumor models, suggesting that the cellular response to RES may regulate the activation of transcriptional factors directed to clusters of genes promoting parallel or overlapping cascades of events inducing cell cycle arrest and eventually apoptosis. However, the role of cell cycle regulation on the extent of RES-induced apoptosis requires further demonstration of the correlation of cell cycle regulation and apoptosis.

The present study also reveals the involvement of mitochondria in RES-induced cell death of RB cells. At present, two major apoptosis pathways have been identified: the intrinsic or mitochondrial pathway and the extrinsic or death receptor–related pathway. The intrinsic pathway involves mitochondria-dependent processes, resulting in cytochrome *c* release and activation of caspase-9. The extrinsic pathway is triggered by the binding of ligands, such as TNF or FasL, to their receptors, leading to the recruitment of adaptor proteins such as FADD and the subsequent activation of procaspase-8.[51] Evidence indicates that RES can induce apoptotic cell death through both mechanisms.[52–54] We concentrated on molecular mechanisms that were triggered early in the intrinsic apoptotic pathway. Accordingly, we observed that RES causes a rapid decrease in $\Delta\Psi_m$, suggesting that the loss of mitochondrial membrane polarization is an early event in RES-induced apoptosis. It has been reported that intact cells may undergo the mitochondrial permeability transition and a loss of $\Delta\Psi_m$ in a fully reversible manner without inducing cell death.[55] Nevertheless, we saw a sustained loss of membrane polarization over an extended period of RES exposure.

After these findings we assessed the effects of RES on the integrity of isolated mitochondria. We observed that much lower concentrations of RES were required to influence a loss

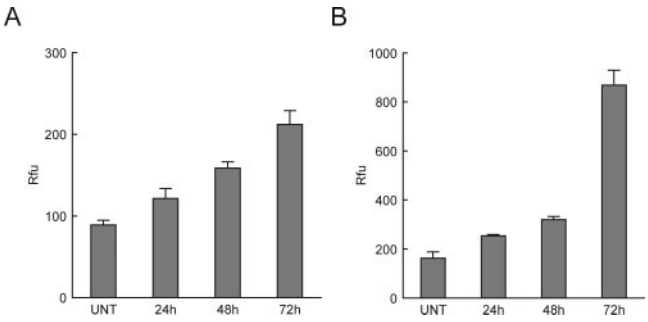

Figure 7. RES activates caspase-9 and caspase-3. Y79 cultures were treated with 50 μM RES for the indicated times, and caspase-9 (**A**) and caspase-3 (**B**) activities were measured spectrofluorometrically using *Ac*-LEHD-AFC and *Ac*-DEVD-AMC as substrates, respectively. The lysates were adjusted for equal protein concentrations using the Bradford assay. (**A**, **B**) Mean ± SD of duplicate samples. Results are representative of one of three independent experiments.

of $\Delta\Psi_m$ in a cell-free system, indicating the possibility of an RES target protein in the mitochondria. These alterations in $\Delta\Psi_m$ were not related to resveratrol inhibition of NQO2, a recently identified target of RES that is cytoplasmic.[36,37] The absence of NQO2 localization in the mitochondria, the lack of its expression in Y79 cells, and the sensitivity of the cells to RES-induced cell death suggest that an alternative primary target of RES may exist in the mitochondria. Identification of a putative RES mitochondrial target could lead to the synthesis of derivatives that are more efficacious growth inhibitory and apoptotic agents in chemoprevention and chemotherapy.

The loss of $\Delta\Psi_m$ commonly accompanies or precedes caspase activation, leading to apoptosis.[45] Consistent with our hypothesis, we observed that the disruption of $\Delta\Psi_m$ by RES appears to precede the activation of caspase-9 and caspase-3. After apoptosis-stimulated mitochondrial membrane permeabilization, cytochrome *c* and other proapoptotic proteins—among them apoptosis-inducing factor, SMAC/Diablo and EndoG—are released into the cytosol.[56] In the present study, RES triggered the release of cytochrome *c* from the mitochondria of Y79 cells, which likely preceded the activation of caspase-9 and caspase-3. Taken together, our results point to a general mechanism of apoptosis induction by RES in retinoblastoma cells that involves a progressive loss of mitochondrial membrane potential and activation of the intrinsic mitochondrial/caspase-9–specific pathway, confirming previous findings from other groups in tumor cell lines of different origin.[54,57,58]

Furthermore, RES could not provoke cytochrome *c* release from isolated mitochondria, suggesting the possible involvement of other cytoplasmic components in RES-induced mitochondrial apoptosis. Although the precise mechanism that mediates the release of cytochrome *c* from the mitochondria is unclear, apoptosis-associated mitochondrial events induced by RES have been shown to be facilitated by the altered expression of apoptotic regulators, such as down-modulation of the antiapoptotic proteins Bcl-2 and Bcl-X_L[59] and the upregulation of proapoptotic Bax and Bak.[60] Moreover, it has been demonstrated that RES triggers Bax-mediated apoptosis through its translocation to the mitochondria in many cancer cell types.[57,60] RES can also induce Bax-independent mitochondrial apoptosis,[60] which may be explained by the redundancy of Bax functions with other proapoptotic Bcl-2 family members. The increased accumulation of reactive oxygen species[61] and the opening of the high-conductance channel called the permeability transition pore (PTP), composed of the adenine-nucleotide translocator (ANT, located in the inner mitochondrial membrane) and the voltage-dependent anion channel (VDAC, found in the outer mitochondrial membrane), have also been suggested to play important roles in mediating cytochrome *c* release.[62,63] Whether the ability of resveratrol to directly target mitochondria and to cause a loss of $\Delta\Psi_m$ in Y79 cells are somehow linked through these protein complexes requires further investigation.

RES has been shown to have a chemopreventive role in vivo in a wide variety of tumors, including skin, liver, colon, breast, lung, and esophageal cancers.[14] Our pilot experiments exploring the effect of daily oral administration of RES in the transgenic mouse model of RB appear promising. Studies with large animal groups are under way. It is hoped our findings will aid in the development of therapeutic strategies for the treatment of retinoblastoma tumors and will indicate that RES may be a useful, nontoxic adjuvant to conventional anticancer therapies for retinoblastoma.

Acknowledgments

The authors thank Joshua Harder for help in preparation of the manuscript.

References

1. Albert DM. Historic review of retinoblastoma. *Ophthalmology*. 1987;94:654–662.
2. Shields CL, Shields JA. Diagnosis and management of retinoblastoma. *Cancer Control*. 2004;11:317–327.
3. Suzuki S, Kaneko A. Management of intraocular retinoblastoma and ocular prognosis. *Int J Clin Oncol*. 2004;9:1–6.
4. Shields JA, Shields CL, Meadows AT. Chemoreduction in the management of retinoblastoma. *Am J Ophthalmol*. 2005;140:505–506.
5. Eng C, Li FP, Abramson DH, et al. Mortality from second tumors among long-term survivors of retinoblastoma. *J Natl Cancer Inst*. 1993;85:1121–1128.
6. Shields CL, Shields JA, Cater J, Othmane I, Singh AD, Micaily B. Plaque radiotherapy for retinoblastoma: long-term tumor control and treatment complications in 208 tumors. *Ophthalmology*. 2001;108:2116–2121.
7. Chan HS, Gallie BL, Munier FL, Beck Popovic M. Chemotherapy for retinoblastoma. *Ophthalmol Clin North Am*. 2005;18:55–63, viii.
8. Murphree AL, Villablanca JG, Deegan WF 3rd, et al. Chemotherapy plus local treatment in the management of intraocular retinoblastoma. *Arch Ophthalmol.* 1996;114:1348–1356.
9. Albert DM, Kumar A, Strugnell SA, et al. Effectiveness of vitamin D analogues in treating large tumors and during prolonged use in murine retinoblastoma models. *Arch Ophthalmol*. 2004;122:1357–1362.
10. Albert DM, Plum LA, Yang W, et al. Responsiveness of human retinoblastoma and neuroblastoma models to a non-calcemic 19-nor vitamin D analog. *J Steroid Biochem Mol Biol*. 2005;97:165–172.
11. Cullinan AE, Lindstrom MJ, Sabet S, Albert DM, Brandt CR. Evaluation of the antitumor effects of herpes simplex virus lacking ribonucleotide reductase in a murine retinoblastoma model. *Curr Eye Res*. 2004;29:167–172.
12. Hurwitz MY, Marcus KT, Chevez-Barrios P, Louie K, Aguilar-Cordova E, Hurwitz RL. Suicide gene therapy for treatment of retinoblastoma in a murine model. *Hum Gene Ther*. 1999;10:441–448.
13. Bradamante S, Barenghi L, Villa A. Cardiovascular protective effects of resveratrol. *Cardiovasc Drug Rev*. 2004;22:169–188.
14. Aggarwal BB, Bhardwaj A, Aggarwal RS, Seeram NP, Shishodia S, Takada Y. Role of resveratrol in prevention and therapy of cancer: preclinical and clinical studies. *Anticancer Res*. 2004;24:2783–2840.
15. Jang M, Cai L, Udeani GO, et al. Cancer chemopreventive activity of resveratrol, a natural product derived from grapes. *Science*. 1997;275:218–220.
16. Aziz MH, Reagan-Shaw S, Wu J, Longley BJ, Ahmad N. Chemoprevention of skin cancer by grape constituent resveratrol: relevance to human disease? *FASEB J*. 2005;19:1193–1195.
17. Provinciali M, Re F, Donnini A, et al. Effect of resveratrol on the development of spontaneous mammary tumors in HER-2/neu transgenic mice. *Int J Cancer*. 2005;115:36–45.
18. Hsieh TC, Wu JM. Differential effects on growth, cell cycle arrest, and induction of apoptosis by resveratrol in human prostate cancer cell lines. *Exp Cell Res*. 1999;249:109–115.
19. Hsieh T, Halicka D, Lu X, et al. Effects of resveratrol on the G(0)-G(1) transition and cell cycle progression of mitogenically stimulated human lymphocytes. *Biochem Biophys Res Commun*. 2002;297:1311–1317.
20. Adhami VM, Afaq F, Ahmad N. Involvement of the retinoblastoma (pRb)-E2F/DP pathway during antiproliferative effects of resveratrol in human epidermoid carcinoma (A431) cells. *Biochem Biophys Res Commun*. 2001;288:579–585.
21. Kim YA, Lee WH, Choi TH, Rhee SH, Park KY, Choi YH. Involvement of p21WAF1/CIP1, pRB, bax and NF-κB in induction of growth arrest and apoptosis by resveratrol in human lung carcinoma A549 cells. *Int J Oncol*. 2003;23:1143–1149.
22. Haider UG, Sorescu D, Griendling KK, Vollmar AM, Dirsch VM. Resveratrol increases serine15-phosphorylated but transcriptionally impaired p53 and induces a reversible DNA replication block in serum-activated vascular smooth muscle cells. *Mol Pharmacol*. 2003;63:925–932.
23. Kim YA, Choi BT, Lee YT, et al. Resveratrol inhibits cell proliferation and induces apoptosis of human breast carcinoma MCF-7 cells. *Oncol Rep*. 2004;11:441–446.

24. Ahmad N, Adhami VM, Afaq F, Feyes DK, Mukhtar H. Resveratrol causes WAF-1/p21-mediated G(1)-phase arrest of cell cycle and induction of apoptosis in human epidermoid carcinoma A431 cells. *Clin Cancer Res*. 2001;7:1466–1473.
25. Don AS, Hogg PJ. Mitochondria as cancer drug targets. *Trends Mol Med*. 2004;10:372–378.
26. Dias N, Bailly C. Drugs targeting mitochondrial functions to control tumor cell growth. *Biochem Pharmacol*. 2005;70:1–12.
27. Fang N, Casida JE. Anticancer action of cube insecticide: correlation for rotenoid constituents between inhibition of NADH: ubiquinone oxidoreductase and induced ornithine decarboxylase activities. *Proc Natl Acad Sci U S A*. 1998;95:3380–3384.
28. Zheng J, Ramirez VD. Inhibition of mitochondrial proton F0F1-ATPase/ATP synthase by polyphenolic phytochemicals. *Br J Pharmacol*. 2000;130:1115–1123.
29. Kipp JL, Ramirez VD. Effect of estradiol, diethylstilbestrol, and resveratrol on F0F1-ATPase activity from mitochondrial preparations of rat heart, liver, and brain. *Endocrine*. 2001;15:165–175.
30. Gledhill JR, Walker JE. Inhibition sites in F1-ATPase from bovine heart mitochondria. *Biochem J*. 2005;386:591–598.
31. Stivala LA, Savio M, Carafoli F, et al. Specific structural determinants are responsible for the antioxidant activity and the cell cycle effects of resveratrol. *J Biol Chem*. 2001;276:22586–22594.
32. Locatelli GA, Savio M, Forti L, et al. Inhibition of mammalian DNA polymerases by resveratrol: mechanism and structural determinants. *Biochem J*. 2005;389:259–268.
33. Szewczuk LM, Forti L, Stivala LA, Penning TM. Resveratrol is a peroxidase-mediated inactivator of COX-1 but not COX-2: a mechanistic approach to the design of COX-1 selective agents. *J Biol Chem*. 2004;279:22727–22737.
34. Subbaramaiah K, Chung WJ, Michaluart P, et al. Resveratrol inhibits cyclooxygenase-2 transcription and activity in phorbol ester-treated human mammary epithelial cells. *J Biol Chem*. 1998;273:21875–21882.
35. Chun YJ, Kim MY, Guengerich FP. Resveratrol is a selective human cytochrome P450 1A1 inhibitor. *Biochem Biophys Res Commun*. 1999;262:20–24.
36. Buryanovskyy L, Fu Y, Boyd M, et al. Crystal structure of quinone reductase 2 in complex with resveratrol. *Biochemistry*. 2004;43:11417–11426.
37. Wang Z, Hsieh TC, Zhang Z, Ma Y, Wu JM. Identification and purification of resveratrol targeting proteins using immobilized resveratrol affinity chromatography. *Biochem Biophys Res Commun*. 2004;323:743–749.
38. Iskander K, Jaiswal AK. Quinone oxidoreductases in protection against myelogenous hyperplasia and benzene toxicity. *Chem Biol Interact*. 2005;153–154:147–157.
39. *ABI Prism 7700 Sequence Detection System: Relative Quantitation of Gene Expression*. User bulletin 2: revision B. Foster City, CA: PE Applied Biosystems; 2001.
40. Reers M, Smith TW, Chen LB. J-aggregate formation of a carbocyanine as a quantitative fluorescent indicator of membrane potential. *Biochemistry*. 1991;30:4480–4486.
41. White RJ, Reynolds IJ. Mitochondrial depolarization in glutamate-stimulated neurons: an early signal specific to excitotoxin exposure. *J Neurosci*. 1996;16:5688–5697.
42. Seong GJ, Park C, Kim CY, et al. Mitomycin-C induces the apoptosis of human Tenon's capsule fibroblast by activation of c-jun N-terminal kinase 1 and caspase-3 protease. *Invest Ophthalmol Vis Sci*. 2005;46:3545–3552.
43. Sun XM, MacFarlane M, Zhuang J, Wolf BB, Green DR, Cohen GM. Distinct caspase cascades are initiated in receptor-mediated and chemical-induced apoptosis. *J Biol Chem*. 1999;274:5053–5060.
44. Green DR, Reed JC. Mitochondria and apoptosis. *Science*. 1998;281:1309–1312.
45. Ly JD, Grubb DR, Lawen A. The mitochondrial membrane potential ($\Delta\Psi_m$) in apoptosis: an update. *Apoptosis*. 2003;8:115–128.
46. da Rocha AB, Lopes RM, Schwartsmann G. Natural products in anticancer therapy. *Curr Opin Pharmacol*. 2001;1:364–369.
47. Ulrich S, Wolter F, Stein JM. Molecular mechanisms of the chemopreventive effects of resveratrol and its analogs in carcinogenesis. *Mol Nutr Food Res*. 2005;49:452–461.
48. Banerjee S, Bueso-Ramos C, Aggarwal BB. Suppression of 7,12-dimethylbenz(a)anthracene-induced mammary carcinogenesis in rats by resveratrol: role of nuclear factor-κB, cyclooxygenase 2, and matrix metalloprotease 9. *Cancer Res*. 2002;62:4945–4954.
49. Kundu JK, Chun KS, Kim SO, Surh YJ. Resveratrol inhibits phorbol ester-induced cyclooxygenase-2 expression in mouse skin: MAPKs and AP-1 as potential molecular targets. *Biofactors*. 2004;21:33–39.
50. Kundu JK, Surh YJ. Molecular basis of chemoprevention by resveratrol: NF-κB and AP-1 as potential targets. *Mutat Res*. 2004;555:65–80.
51. Green DR. Apoptotic pathways: ten minutes to dead. *Cell*. 2005;121:671–674.
52. Fulda S, Debatin KM. Resveratrol-mediated sensitisation to TRAIL-induced apoptosis depends on death receptor and mitochondrial signalling. *Eur J Cancer*. 2005;41:786–798.
53. Delmas D, Rebe C, Lacour S, et al. Resveratrol-induced apoptosis is associated with Fas redistribution in the rafts and the formation of a death-inducing signaling complex in colon cancer cells. *J Biol Chem*. 2003;278:41482–41490.
54. Dorrie J, Gerauer H, Wachter Y, Zunino SJ. Resveratrol induces extensive apoptosis by depolarizing mitochondrial membranes and activating caspase-9 in acute lymphoblastic leukemia cells. *Cancer Res*. 2001;61:4731–4739.
55. Minamikawa T, Williams DA, Bowser DN, Nagley P. Mitochondrial permeability transition and swelling can occur reversibly without inducing cell death in intact human cells. *Exp Cell Res*. 1999;246:26–37.
56. Henry-Mowatt J, Dive C, Martinou JC, James D. Role of mitochondrial membrane permeabilization in apoptosis and cancer. *Oncogene*. 2004;23:2850–2860.
57. Jiang H, Zhang L, Kuo J, et al. Resveratrol-induced apoptotic death in human U251 glioma cells. *Mol Cancer Ther*. 2005;4:554–561.
58. Zunino SJ, Storms DH. Resveratrol-induced apoptosis is enhanced in acute lymphoblastic leukemia cells by modulation of the mitochondrial permeability transition pore. *Cancer Lett*. In press.
59. Pozo-Guisado E, Merino JM, Mulero-Navarro S, et al. Resveratrol-induced apoptosis in MCF-7 human breast cancer cells involves a caspase-independent mechanism with downregulation of Bcl-2 and NF-κB. *Int J Cancer*. 2005;115:74–84.
60. Mahyar-Roemer M, Kohler H, Roemer K. Role of bax in resveratrol-induced apoptosis of colorectal carcinoma cells (serial online). *BMC Cancer*. 2002;2:27.
61. Atlante A, Calissano P, Bobba A, Azzariti A, Marra E, Passarella S. Cytochrome *c* is released from mitochondria in a reactive oxygen species (ROS)-dependent fashion and can operate as a ROS scavenger and as a respiratory substrate in cerebellar neurons undergoing excitotoxic death. *J Biol Chem*. 2000;275:37159–37166.
62. Petronilli V, Penzo D, Scorrano L, Bernardi P, Di Lisa F. The mitochondrial permeability transition, release of cytochrome *c* and cell death. correlation with the duration of pore openings in situ. *J Biol Chem*. 2001;276:12030–12034.
63. Martinou JC, Desagher S, Antonsson B. Cytochrome *c* release from mitochondria: all or nothing. *Nat Cell Biol*. 2000;2:E41–E43.